

## Threshold Behavior near an Electronic Shape Resonance: Analysis of the He( $2^3P$ ) Threshold in He $^-$ Photodetachment and Determination of the He( $2^3S$ ) Electron Affinity

J. R. Peterson, Y. K. Bae, and D. L. Huestis

*Molecular Physics Department, SRI International, Menlo Park, California 94025*

(Received 11 April 1985)

He $^-$  photodetachment cross sections near the He( $2^3P$ ) threshold have been measured and analyzed. The data were found to deviate rapidly from the Wigner threshold law because of the strong influence of the nearby  $4P^e$  shape resonance. A modified formula has been derived, which accounts for this effect. It successfully fits the data not only in the threshold region but over the resonance itself. The threshold data yield an electron affinity for He( $2^3S$ ) of  $77.5 \pm 0.8$  meV, in agreement with the accurate calculations of Bunge and Bunge.

PACS numbers: 32.80.Fb, 34.80.Dp, 35.10.Hn

The energy dependence of cross sections near the thresholds of opening reaction channels has been of interest for years, as has their behavior near scattering resonances. However, little attention has been given to the combined effects. We describe here, for the first time, the effects of a shape resonance on the threshold behavior of opening-channel cross sections.

In the first measurements near the large  $1s2p^24P^e$  shape resonance in He $^-$  photodetachment<sup>1</sup> we were unable to operate the cw dye laser far enough into the infrared to reach the He( $2^3P$ ) +  $\epsilon p$  threshold at  $\lambda = 1015$  nm for a determination of the He( $1s2s2p4P^o$ ) binding energy. Improvements in both the experimental arrangement and the laser operation have led to a great reduction in the uncertainties of the data in the resonance region and have allowed measurements down to the  $2^3S$  threshold. The data reveal the form of a shape resonance in unprecedented detail. In the threshold region the cross sections deviate rapidly from the Wigner threshold law,<sup>2</sup> preventing its use in locating the He( $2^3P$ ) threshold. Evidently, the presence of the nearby resonance strongly affects the cross sections very close to the threshold.

To account for these effects we have derived a parametric expression that successfully describes not only the threshold region but the resonance as well. Least-squares fits to the data yield an accurate value of the threshold energy, as well as parameters that closely approximate the energy and width of the resonance. This Letter is concerned primarily with the behavior of opening-channel cross sections in the vicinity of a  $p$ -wave shape resonance, and with the determination of the He( $2^3S$ ) electron affinity (EA). A more complete description of the  $4P^e$  resonance itself and of the experiment will be given elsewhere.<sup>3</sup>

According to Wigner's threshold law,<sup>2</sup> derived for short-ranged opening channels whose interaction energies fall off faster than  $r^{-2}$ , the photodetachment cross section  $\sigma$  near the threshold should behave as

$$\sigma \sim k^{2l+1}, \quad (1)$$

where  $k$  and  $l$  are, respectively, the linear and angular momenta of the outgoing electron. Accordingly, for this  $p$ -wave channel, the energy dependence near threshold should be given by

$$\sigma \sim (E - E_0)^{3/2}, \quad (2)$$

where  $E$  is the photon energy and  $E_0$  is the threshold energy. In attempting to fit our data by this form, we found that the value of  $E_0$  determined by the least-squares fitting procedure was never independent of the number of data included, and when the fitted curve of Eq. (2) was compared to the data, it was apparent that the increasing oscillator strength due to the resonance affected the cross section very close to the threshold, and the Wigner law could not be used. Although initially frustrating, this finding was not entirely surprising because of our prior knowledge<sup>1,4</sup> that the resonance is located only  $\sim 10$  meV above the threshold and has a width (FWHM) of  $\sim 7$  meV. The deviations from the Wigner law are much greater than would be expected from polarization forces, whose effects were formulated by O'Malley.<sup>5</sup> Rapid deviations from the Wigner law have already been found in the photodetachment of alkali-metal negative ions above the first outgoing  $s$ -wave thresholds. These were observed experimentally<sup>6,7</sup> in Rb $^-$  and Cs $^-$ , and in *ab initio* calculations<sup>8</sup> on K $^-$ . These thresholds are near Feshbach resonances. Nesbet<sup>9</sup> has expressed a multichannel theory for  $s$ -wave-threshold resonance structure; however, we are unaware of any previous formulation of a threshold law that explicitly includes the effects of a shape resonance.<sup>10</sup> Subsequent to the analysis of shape-resonance effects described here, we have applied Nesbet's theory to explain deviations from the Wigner law for an  $s$ -wave cusp, which we observed experimentally in Li $^-$  photodetachment<sup>11</sup> and which has also been found in *ab initio* calculations.<sup>8</sup> We found that photodetachment near the opening Li( $2p$ ) +  $\epsilon s$  channel threshold is affected by a virtual state, and derived a modified Wigner cusp form.<sup>11</sup>

We present here one approach to the shape-resonance problem, using standard scattering theory.

We have also found that essentially the same results can be reached by other methods.

The total cross section for the photoexcitation of a single opening detachment channel may be written as

$$\sigma_l \sim k |M_l|^2, \quad (3)$$

where  $M_l$  is the dipole matrix element connecting the initial (negative ion) and final (atom plus electron) states.  $M_l$  contains only contributions from a small finite region of space because of the localization of the initial wave function. Since (near threshold) the asymptotic energy of the final-state wave function is infinitesimal compared to the interaction energy in this localized region, the only characteristic of the *local* final-state wave function that is sensitive to small variations of the asymptotic energy is the amplitude, which is proportional to the inverse of the (volume) normalization factor of the asymptotic wave function. Following this idea, O'Malley<sup>5</sup> factored  $M_l$  as

$$M_l = N_l^{-1} M', \quad (4)$$

where  $N_l$  is the normalization factor of the asymptotic final-state electron wave function and  $M'$  is a constant to lowest order in  $k^2$ . O'Malley<sup>5</sup> also noted, with reference to Gillespie,<sup>12</sup> that  $N_l$  is connected to the Jost function  $f_l(k)$  by

$$N_l = |f_l(k)| k^{-l}, \quad (5)$$

and we point out that the Jost function is related to the scattering matrix  $S_l(k)$  by<sup>13</sup>  $S_l(k) = f_l(-k)/f_l(k)$ . Now, from Eqs. (3)–(5), we see that the cross section of the new opening channel near its threshold may be written as

$$\sigma_l \sim k^{2l+1} |f_l(k)|^{-2}. \quad (6)$$

The following arguments are based on standard scattering theory.<sup>13</sup> If there is no zero of  $f_l(k)$  in the complex  $k$  plane (corresponding to a pole of the scattering matrix, i.e., a resonance) near the threshold, then  $f_l(k)$  can be regarded as constant over a small range of  $k \sim 0$ , and the cross section Eq. (6) follows the Wigner threshold law, Eq. (1). However, if there is a zero of  $f_l(k)$  (a resonance) near the threshold, as often occurs in electron scattering at energies near excited neutral states, then  $f_l(k)$  can vary strongly, and Eq. (6) deviates from the Wigner law very close to the threshold.

To see how  $f_l(k)$  depends on  $k$  when it has a zero close to  $k=0$ , we assume<sup>13</sup> that the attractive interaction potential (correlation energy)  $\lambda V(r)$  in the final state is short ranged as in electron-atom scattering or photodetachment, neglecting the polarization potential.<sup>14</sup> The parameter  $\lambda$  represents the strength of the potential, and if  $\lambda = \lambda_0$ , the zero of  $f_l(k)$  occurs at  $k=0$ . We suppose that  $\lambda - \lambda_0$  is small, and that near

$k=0$ ,  $f_l(k)$  can be expanded as<sup>13</sup>

$$f_l(k) \sim \beta_l k^2 + i\gamma_l k^{2l+1} + \eta_l(\lambda - \lambda_0) \\ + \text{higher-order terms}, \quad (7)$$

where  $\beta_l$ ,  $\gamma_l$ , and  $\eta_l$ , are real constants that depend only on the shape of the potential<sup>13</sup> (not on its strength).

For  $l=0$ , if  $\lambda > \lambda_0$ , the potential is strong enough to create a bound-state (Feshbach) resonance and the corresponding zero lies on the positive imaginary axis of the  $k$  plane. As  $\lambda$  decreases, the zero moves down the imaginary axis and finally reaches  $k=0$  when  $\lambda = \lambda_0$ . If  $\lambda$  becomes less than  $\lambda_0$ , then the zero moves onto the negative axis and is referred to as a virtual state. On the other hand, for  $l \geq 1$ , a bound state has two zeros located on the positive and negative imaginary axes, which move toward  $k=0$  as  $\lambda \rightarrow \lambda_0$ . If  $\lambda$  becomes less than  $\lambda_0$  these two zeros leave the imaginary axis in opposite directions, moving into the lower half of the  $k$  plane, and the zero on the right bears a shape resonance at  $E > E_0$ . Physically this means simply that in order to support a shape resonance when  $\lambda < \lambda_0$ , the centrifugal barrier (produced when  $l \geq 1$ ) is necessary. The scattering phase shift increases through  $(n + \frac{1}{2})\pi$  as the energy passes through both bound and shape resonances, but not for virtual states.

We only consider the case of  $l=1$ . The cases where  $l \geq 2$  are more complicated. For the  $l=1$  case, if we keep the three lowest-order terms of Eq. (7) and combine them into Eq. (6) we have

$$\sigma \sim k^3 / [(k^2 - k_1^2)^2 + \gamma^2 k^6], \quad (8)$$

where  $k_1^2 = -\eta_1(\lambda - \lambda_0)/\beta_1$  and  $\gamma = \gamma_1/\beta_1$ . The denominator of Eq. (8) is cubic in  $k^2$ , and further manipulation allows its transformation into

$$(k^2 + A) [(k^2 - k_R^2)^2 + \Gamma^2], \quad (9)$$

where  $A$  is a constant (which we found in this work to be much larger than  $k^2$ ). Here,  $k_R^2/2$  and  $\Gamma$  are the real and imaginary parts of the resonance zero in the complex energy plane, and thus are the position and width of the resonance. If, for small  $k$ , we approximate  $k^2 + A$  as a constant, then we can transform Eq. (8) into

$$\sigma \sim k^3 / [(k^2 - k_R^2)^2 + \Gamma^2], \quad (10)$$

which is simply a product of the Wigner threshold law and the Breit-Wigner resonance formula. It also can be seen that the denominator of Eq. (8) is similar to the Breit-Wigner resonance form but the decay rate is given by  $\gamma k^3$ . In this case,  $k_1^2/2$  and  $\gamma k_1^3$  only approximate the position and width of the resonance.

As we mentioned above, equivalent forms can be derived in other ways. Our first approach<sup>15</sup> was to model photodetachment via a shape resonance above a

square well. The problem was easily solved for  $l=1$ , yielding Eq. (10) with  $\Gamma$  an undetermined but slowly varying function of energy. On the other hand, Watanabe<sup>16</sup> has made an extensive treatment of five doubly excited states of  $\text{He}^-$ , using hyperspherical coordinates (and multichannel quantum-defect theory). Although he was not able to determine whether  $\text{He}^- (^4P^e)$  was a Feshbach or shape resonance, he calculated photodetachment cross sections for both cases. While preparing the final version of our manuscript we found that by using his approximation for the energy-normalized quantum defect near the resonance, Eq. (53), in his Eq. (54a), which approximates the cross section near the resonance, the latter can be reduced to the form of our Eq. (8).

As details of the experimental technique and apparatus are given elsewhere,<sup>3</sup> only brief descriptions are presented here.  $\text{He}^-$  ions were formed from a 2-keV momentum-analyzed  $\text{He}^+$  beam by two-step electron capture in Cs vapor. The three  $\text{He}^{+,0,-}$  charge components were separated by an electrostatic quadrupole whose ion-optical properties and geometry facilitate a coaxial laser-ion-beam interaction. Two 1.4-mm (horizontal)  $\times$  2.2-mm (vertical) apertures at the exit of the first quadrupole and the entrance of the second quadrupole served to define the field-free interaction region, as both laser and ion beams were initially larger than the apertures and essentially uniform over its area. The neutrals formed from either autodetachment or photodetachment impinged upon the electrically conductive surface of a glass plate to pro-

duce secondary electrons which were accelerated to a channel electron multiplier for detection. The laser optics and the dye (IR 140) were the same as we used previously,<sup>1</sup> but the dye performance was improved by doubling the concentration of the dimethyl-sulfoxide solvent. As the laser and ion beams both effectively and uniformly filled the beam-defining apertures, the total photodetachment cross section  $\sigma_T$  is approximated very well by

$$\sigma_T = sav/i^- i_p d, \quad (11)$$

where  $s$  is the photodetachment neutral-product count rate,  $a$  the area of the defining aperture,  $v$  the velocity of the  $\text{He}^-$  ion,  $i^-$  the  $\text{He}^-$  current estimated from the count rate of autodetached He neutrals,  $i_p$  the equivalent photon current, and  $d$  the length of the interaction region.

Figure 1 shows a least-squares fit of the first seven data by the Wigner threshold law, Eq. (1). As a result of the strong effects of the shape resonance the cross section rapidly deviates from the Wigner law. Because of this rapid deviation and the large uncertainties of the data near the threshold (where the laser was weak), the threshold value obtained by fitting the data with the Wigner threshold law increases substantially when the number of data points used for fitting increases. On the other hand, both Eqs. (8) and (10) gave quite good fits, not only to the threshold data as shown in Fig. 1, but to the entire resonance peak as well, as is seen in Fig. 2.

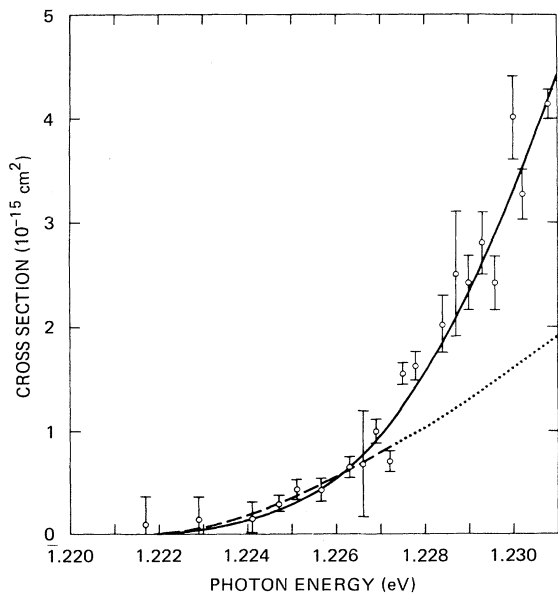


FIG. 1. Least-squares fits of near-threshold data curve: dashed curve, Wigner threshold law; solid curve, modified form.

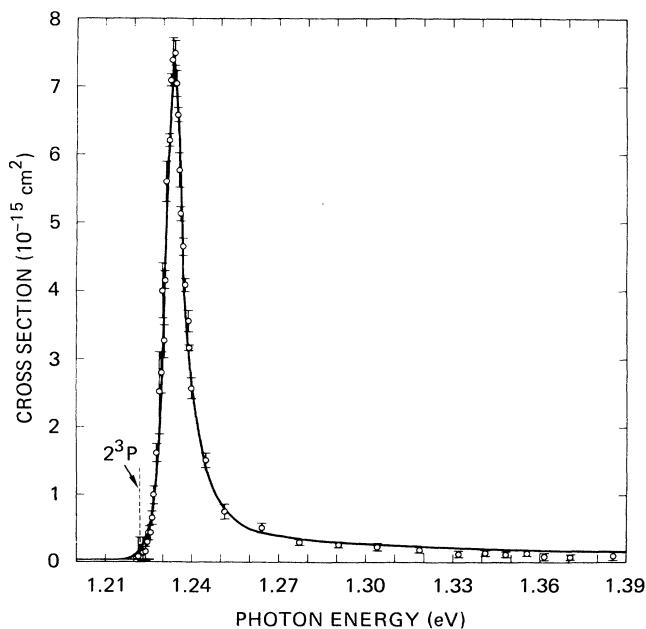


FIG. 2. Least-squares fit of all data (within 170 meV of threshold) by Eq. (8). The fit of Eq. (10) is indistinguishable except in the high-energy tail.

TABLE I. Threshold and resonance energies (in millielectronvolts) obtained from data fits.

Equation	He( $2^3P$ )	He( $2^3S$ )	Resonance parameters	
	threshold $E_0$	EA	Position above $E_0$	Width
(8)	$1222.0 \pm 0.8$	$77.5 \pm 0.8$	$k_1^2/2 = 12.3 \pm 0.3$	$\gamma k_1^3 = 8.6 \pm 0.4$
(10)	$1222.1 \pm 1.0$	$77.6 \pm 1.0$	$k_R^2/2 = 10.8 \pm 0.3$	$\Gamma = 7.4 \pm 0.3$

Above the  $2^3P$  threshold,  $\sigma_T$  consists of a small contribution  $\sigma_0$  from the continuum of the  $2^3S + \epsilon(s+d)$  channel, which is estimated from our earlier data<sup>1</sup> to be  $3.5 \times 10^{-17}$  cm<sup>2</sup> at the  $2^3P$  threshold, and we assumed it to be constant over the small energy range of this work. This background level is shown in Fig. 2 as the short horizontal line near the threshold and is very small compared to the  $2^3P + \epsilon p$  cross section  $\sigma = \sigma_T - \sigma_0$ , even in the threshold region shown in Fig. 1. The resonance parameters in Eqs. (8) and (10) were first established by fitting all data within 170 meV of threshold. This fit is shown in Fig. 2. We note that  $k^2/2 = h\nu - E_0$ , where  $h\nu$  and  $E_0$  are the photon and threshold energies. All the data were weighted according to the inverse square of their experimental standard deviations. Equation (8) gave  $k_1^2/2 + E_0 = 1234.3$  meV and  $\gamma k_1^3 = 8.6$  meV; Eq. (10) yielded  $k_R^2/2 + E_0 = 1232.9$  meV and  $\gamma = 7.4$  meV. Next,  $k_1$ ,  $\gamma$ ,  $k_R$ , and  $\Gamma$  were held fixed and only the data within 10 meV of threshold were used to find  $E_0$ . This fit is shown in Fig. 1. The threshold given by Eq. (8) is shown in Fig. 2. These threshold fits yielded the electron affinity of He( $2^3S$ ) to be  $77.5 \pm 0.8$  meV from Eq. (8) and  $77.6 \pm 1.0$  meV from Eq. (10). The uncertainties have been determined by combining the uncertainties in the fitting parameters [0.7 meV for Eq. (8) and 0.9 meV for Eq. (10)] and laser wavelength calibration (0.2 meV). The uncertainties in the threshold data arose primarily from the weak output of the dye laser near its own operational threshold. A summary of the results is given in Table I. These results are in excellent agreement with the electron affinity of  $77.51 \pm 0.04$  meV recently calculated by Bunge and Bunge.<sup>17</sup>

In summary, we have measured and analyzed He<sup>-</sup> photodetachment cross sections near the He( $2^3P$ ) threshold which is affected strongly by the  $4P\epsilon$  shape resonance. We derived a modified formula from the scattering theory which fits not only the threshold region but the entire resonance. From the fittings the electron affinity of He( $2^3S$ ) has been determined to be  $77.5 \pm 0.8$  meV, in excellent agreement with the calculation by Bunge and Bunge.

Because shape resonances are "bound" only by centrifugal barriers connected with opening channels, it is

their nature to be located close to thresholds, with widths comparable to the separations. Therefore, it is quite likely that they will always have a strong influence in the threshold behavior.

We are grateful to Dr. T. F. O'Malley for helpful theoretical discussions, and to Dr. M. J. Coggiola for assistance on some experimental problems. This work was supported by the National Science Foundation under Grants No. PHY 81-11912 and No. PHY 84-10980, and by the U. S. Air Force Office of Scientific Research under Contract No. F49620-82-K-0030.

<sup>1</sup>J. R. Peterson, M. J. Coggiola, and Y. K. Bae, Phys. Rev. Lett. **50**, 664 (1983).

<sup>2</sup>E. P. Wigner, Phys. Rev. **73**, 1002 (1948).

<sup>3</sup>J. R. Peterson, Y. K. Bae, and M. J. Coggiola, to be published.

<sup>4</sup>A. V. Hazi and K. Reed, Phys. Rev. A **24**, 2269 (1981).

<sup>5</sup>T. F. O'Malley, Phys. Rev. **137**, A1668 (1965).

<sup>6</sup>P. Frey, M. Lawen, F. Breyer, H. Klar, and H. Hotop, Z. Phys. A **304**, 155 (1982).

<sup>7</sup>R. D. Mead, P. A. Schultz, and W. C. Lineberger, unpublished.

<sup>8</sup>D. L. Moores and D. W. Norcross, Phys. Rev. A **10**, 1646 (1974).

<sup>9</sup>R. K. Nesbet, J. Phys. B **13**, L193 (1980).

<sup>10</sup>J. P. Connerade, J. Phys. B **17**, L173 (1984), has obtained fits to  $l=3$  photoionization shape resonances from the scattering phase shifts of a square-well potential, but did not treat the threshold region explicitly.

<sup>11</sup>Y. K. Bae and J. R. Peterson, in Proceedings of the Thirty-Seventh Gaseous Electronics Conference, Boulder, Colorado, October 1984 (unpublished), and Phys. Rev. A (to be published).

<sup>12</sup>J. Gillespie, Phys. Rev. **135**, A75 (1964).

<sup>13</sup>J. R. Taylor, *Scattering Theory* (Wiley, New York, 1972).

<sup>14</sup>The effects of polarization forces on the Wigner law have been treated by O'Malley (Ref. 5). We assume here that they generally will have little effect compared to a nearby resonance; however this may not always be the case, if the resonance is weak or distant.

<sup>15</sup>J. R. Peterson, Y. K. Bae, M. J. Coggiola, and D. L. Huestis, Am. Soc. Phys. **29**, 823 (1984).

<sup>16</sup>S. Watanabe, Phys. Rev. A **25**, 2074 (1982).

<sup>17</sup>A. V. Bunge and C. F. Bunge, Phys. Rev. A **30**, 2179 (1984).